Inorg. Chem. **2008**, *47*, 11561−11569

Synthesis and Characterization of Cyclotriphosphazenes Containing Silicon as Single Solid-State Precursors for the Formation of Silicon/Phosphorus Nanostructured Materials

Carlos Díaz,*,† Maria Luisa Valenzuela,† Daniel Bravo,† Vladimir Lavayen,‡ and Colm O'Dwyer§

Department of Chemistry, Faculty of Science, Universidad of Chile, Casilla 653, Santiago Chile, ICEX, Universidade Federal de Minas Gerais, Av. Antonio Carlos 6623, Pampulha CP 70, Belo Horizonte, Brasil, and Department of Physics, and Materials and Surface Science Institute, University of Limerick, Limerick, Ireland

Received May 29, 2008

The synthesis and characterization of new organosilicon derivatives of $N_3P_3Cl_6$, $N_3P_3[NH(CH_2)_3Si(OEt)_3]_6$ (**1**), $N_3P_3[NH(CH_2)_3Si(OEt)_3]_3[NCH_3(CH_2)_3CN]_3$ (**2**), and $N_3P_3[NH(CH_2)_3Si(OEt)_3]_3[HOC_6H_4(CH_2)CN]_3$ (**3**) are reported. Pyrolysis of **1**, **2**, and **3** in air and at several temperatures results in nanostructured materials whose composition and morphology depend on the temperature of pyrolysis and the substituents of the phosphazenes ring. The products stem from the reaction of SiO_2 with P_2O_5, leading to either crystalline $Si_5(PO_4)_6O$, SiP_2O_7 or an amorphous phase as the glass $Si_5(PO_4)_6O/3SiO_2 \cdot 2P_2O_5$, depending on the temperature and nature of the trimer precursors. From **1** at 800 °C, core−shell microspheres of SiO_2 coated with $Si_5(PO_4)_6O$ are obtained, while in other cases, mesoporous or dense structures are observed. Atomic force microscopy examination after deposition of the materials on monocrystalline silicon wafers evidences morphology strongly dependent on the precursors. Isolated islands of size ∼9 nm are observed from **1**, whereas dense nanostructures with a mean height of 13 nm are formed from **3**. Brunauer−Emmett−Teller measurements show mesoporous materials with low surface areas. The proposed growth mechanism involves the formation of cross-linking structures and of vacancies by carbonization of the organic matter, where the silicon compounds nucleate. Thus, for the first time, unique silicon nanostructured materials are obtained from cyclic phosphazenes containing silicon.

Introduction

Silicon-based compounds are of immense technological importance, from monocrystalline silicon as the basis of the digital age to polycrystalline silicon in photovoltaic devices.[1] The fabrication and study of silica (SiO_2) has received considerable attention in recent years, largely due to its potential in diverse applications (e.g., catalysis[2,3]) other than in silicon-based electronic architectures. Its nanoscale counterparts have enjoyed a resurgence in interest due in part to the fundamental differences in properties between the nanoscale and bulk material.[4]

Nanoparticles of silicon are known to exhibit particle-size-dependent optical and electronic properties. Such properties are thought to have important applications in the development of optoelectronic devices and as solubilized crystalline silicon.[5] Also, nanostructured silica has received considerable attention due to exhibited potential in applications such as photonic crystals, nanomicroelectronics/photonics, bionanotechnology, and nanocatalysis.[6]

Several preparation methods of silicon nanoparticles have been reported, the majority facilitated by solution reduction of $SiCl_4$.[7] On other hand, silicon dioxide is generally prepared

* To whom correspondence should be addressed. Phone: 56-2-9787367. Fax: 56-2-2713888. E-mail: cdiaz@uchile.cl.
† Universidad of Chile.
‡ Universidade Federal de Minas Gerais.
§ University of Limerick.

(1) (a) Shah, A.; Torres, P.; Tscharner, R.; Wyrsch, N.; Keppner, H. *Science* **1999**, *285*, 69. (b) Sze, S. M. *Physics of Semiconductor Devices*; John Wiley & Sons: New York, 1985.
(2) Stein, A.; Helde, B. Y.; Schrodern, R. C. *Adv. Mater.* **2000**, *12*, 1403.
(3) Kageyama, K.; Tamazawa, Y. I.; Aida, T. *Science* **1999**, *285*, 2113.
(4) Rao, C. N.; Muller, A.; Cheetham, A. K. *The Chemistry of Nanomaterials*; Wiley-VCH: New York, 2003.
(5) Tsybeskov, L. *MRS Bull.* **1998**, *23*, 33.
(6) (a) Anwander, R. *Chem. Mater.* **2001**, *13*, 4419. (b) Fenollosa, R.; Meseguer, F.; Tymczenko, M. *Adv. Mater.* **2008**, *20*, 95.
(7) Baldwin, R. K.; Pettigrew, K. A.; Garno, J. C.; Power, Ph. P.; Yiu, G.; Kauzlarich, S. M. *J. Am. Chem. Soc.* **2002**, *124*, 1150.

10.1021/ic8009805 CCC: $40.75
Published on Web 11/01/2008

Scheme 1. Schematic Representation of the SSPO Method

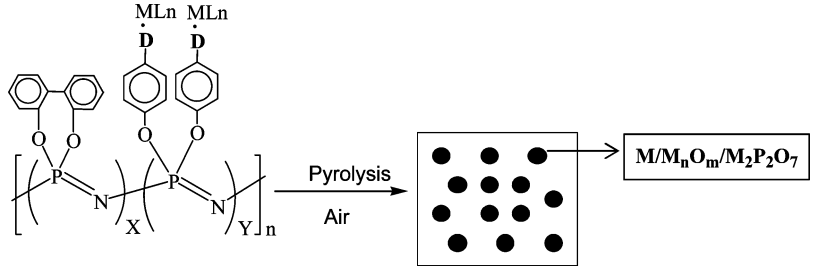

Scheme 2. Structural Formulae of the New Organosilicon Cyclotriphosphazenes **1**, **2**, and **3**

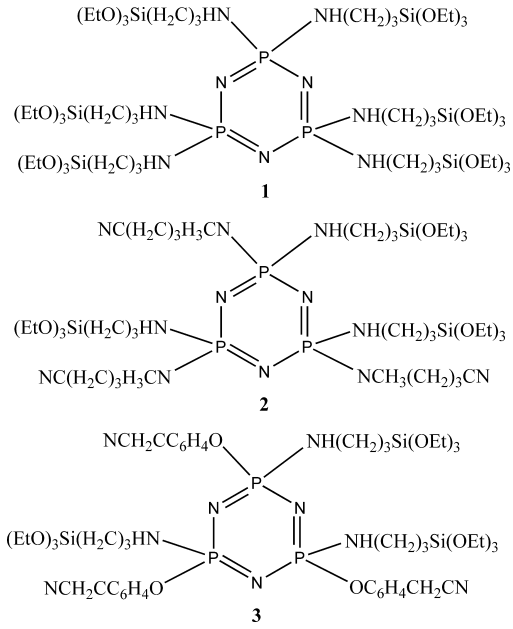

by the sol−gel method.[8,9] The majority of methods for obtaining either Si or silica nanoparticles are based on solutions using polymers as a stabilizer. Apart from Si and SiO_2 nanoparticles, few other Si-containing nanoparticles have been reported.

We have recently reported[10] a solid-state method of obtaining metallic M°, M_xO_y, and $M_x(P_2O_7)_y$ nanoparticles by solid-state pyrolysis of polyphosphazene-containing organometallic derivatives (solid-state pyrolysis of organophosphazene/organometallic, SSPO method), summarized in Scheme 1.

Because of the importance of obtaining silicon, silica, and silicon-containing nanostructured materials in their solid states, we have successfully developed a synthetic method of preparing solid-state silicon-containing nanomaterials from the pyrolysis of organosilicon derivatives of cyclotriphosphazenes; the formula structure of each organosilicon precursor is outlined in Scheme 2.

Although polyphosphazenes have been previously used to stabilize gold nanoparticles in solution,[11] no examples of the stabilization of metal nanoparticles by cyclic phosphazenes in solution or in the solid state have been reported. We previously reported on the synthesis and characterization of organometallic derivatives of cyclotriorganophosphazene,[12] and here we detail the synthetic method and characterize several new organosilicon derivatives of cyclotriphosphazenes and a study of their pyrolysis. Although several cyclotriphosphazenes containing silicon substituents have been prepared by Allcock et al.,[13] to the best of our knowledgement, the synthesis of precursors **1**−**3** has never been reported.

For the first time, nanostructured silicon-containing materials are obtained from the solid-state pyrolysis of silicon derivatives of cyclotriphosphazenes.

Experimental Section

All reactions were carried out under dinitrogen using standard Schlenk techniques. Infrared (IR) spectra were recorded on an FT-IR Perkin-Elmer 2000 spectrophotometer. Solvents were dried and purified using standard procedures using $N_3P_3Cl_6$, $[NBu_4]Br$, K_2CO_3, $H_2N(CH_2)_3Si(OEt)_3$, $HN(CH_3)(CH_2)_3CN$, and $HOC_6H_4CH_2CN$ (Sigma-Aldrich). Nuclear magnetic resonance (NMR) spectra were obtained using a Bruker AC-300 instrument with $CDCl_3$ as the solvent, unless otherwise stated. ^1H and $^{13}C\{^1H\}$ NMR are given in δ relative to tetramethylsilane. $^{31}P\{^1H\}$ spectra are given in δ relative to external 85% aqueous H_3PO_4. Coupling constants are in hertz. Thermogravimetric analysis (TGA) and differential scanning calorimetry (DSC) measurements were performed on a Mettler TA 4000 instrument and Mettler DSC 300 differential scanning calorimeter, respectively. The trimer samples were heated at a rate of 10 °C min^{-1} from ambient temperature to 1000 °C under a constant flow of nitrogen.

X-ray diffraction (XRD) was carried out at room temperature on a Siemens D-5000 diffractometer with $\theta-2\theta$ geometry. The XRD data were collected using Cu Kα radiation (40 kV and 30 mA). Scanning electron microscopy (SEM) and energy dispersive X-ray analysis were acquired with a JEOL 5410 SEM with a NORAN Instrument microprobe transmission microscope. Trans-

(8) Soler-Ilhia Sanchez, G.; Lebean, B.; Patasin, Y. *Chem. Rev.* **2002**, *102*, 4093.
(9) Moller, K.; Bein, T. *Chem. Rev.* **1998**, *10*, 2950.
(10) (a) Díaz, C.; Valenzuela, M. L. *J. Chil. Chem. Soc.* **2005**, *50*, 417. (b) Díaz, C.; Valenzuela, M. L. *Macromolecules* **2006**, *39*, 103. (c) Díaz, C.; Castillo, P.; Valenzuela, M. L. *J. Cluster Sci.* **2005**, *16*, 515. (d) Díaz, C.; Valenzuela, M. L. *J. Inorg. Organomet. Polym.* **2006**, *16*, 123.
(11) (a) Yung, Y.; Kmecko, T.; Chaypool, Ch. L.; Zhang, H.; Wisian-Nelson, P. *Macromolecules* **2005**, *38*, 2122. (b) Walker, C. H.; St. John, Y. V.; Wisian-Neilson, P. *J. Am. Chem. Soc.* **2001**, *123*, 3846. (c) Olshavsky, M. A.; Allcock, H. R. *Chem. Mater.* **1997**, *9*, 1367.
(12) (a) Diaz, C.; Barbosa, M.; Godoy, Z. *Polyhedron* **2004**, *23*, 1027. (b) Díaz, C.; Izquierdo, I.; Mendizábal, E.; Yutronic, N. *Inorg. Chim. Acta* **1999**, *294*, 207. (c) Díaz, C.; Izquierdo, I. *Polyhedron* **1999**, *18*, 1479.
(13) (a) Allcock, H. R.; Kuhercik, S. E. *J. Inorg. Organomet. Polym.* **1995**, *5*, 307. (b) Allcock, H. R.; Kuhercik, S. E. *J. Inorg. Organomet. Polym.* **1996**, *6*, 1. (c) Allcock, H. R.; Brennan, D. J. *J. Organomet. Chem.* **1988**, *341*, 231.

mission electron microscopy (TEM) was carried out on a JEOL SX100 TEM and on a JEOL JEM-2011 operating at 200 kV. The finely powered samples were dispersed in *n*-hexane and dropped on a conventional carbon-coated copper grid dried under a lamp. The pyrolysis experiments were carried out by pouring a weighed portion (0.05−0.15 g) of the organometallic trimer into aluminum oxide boats placed in a tubular furnace (Lindberg/Blue Oven model STF55346C-1) under a flow of air, heated from 25 to 300 °C and then to 800 °C, and annealed for 2 h. The heating rate was 10 °C min^{-1} under an air flow of 200 mL min^{-1}. Brunauer−Emmett−Teller (BET) surface areas were calculated from the adsorption isotherm, using a Micromeritics ASP 2010 instrument. The pore size distribution was evaluated using the Bopp−Jancso−Heinzinger method.

Atomic force microscopy (AFM) measurements were performed using a Veeco Explorer AFM in the tapping mode. Roughness, feature size, and image treatments were conducted using the accompanying software. Suitable depositions were obtained by dissolving the trimers **1**, **2**, and **3** in dichloromethane and dropping them on a silicon wafer, followed by evaporation of the solvent at room temperature. Subsequent pyrolysis was conducted at 800 °C.

Synthesis of $N_3P_3[NH(CH_2)_3Si(OEt)_3]_6$ (1). A solution of $N_3P_3Cl_6$ (5 g, 14.4 mmol) in toluene (20 mL) was added dropwise to 3-aminopropyl(triethoxy)silane (21.03 g, 95 mmol) and triethylamine (10.57 g, 105 mmol) in toluene (50 mL) at room temperature. The reaction mixture was heated under reflux for 4 h. During this time, a white precipitate formed. The precipitate was removed by filtration. The solvent was evaporated from the filtrate, and the 3-aminopropyl(triethoxy)silane and triethylamine residues were evaporated under a vacuum at 100 °C. The product was obtained as an opaque liquid in quantitative yield.

Elem anal. calcd for $C_{54}H_{132}N_9O_{18}P_3Si_6$ (found): C, 44.5 (40.00); H, 9.13 (9.60); N, 8.65 (8.26). ^{31}P NMR (ppm, $CDCl_3$): 0.72. ^1H NMR (ppm, $CDCl_3$): δ 1.18 m, 72 H, $[(CH_2)_3Si(OCH_2CH_3)_3]_6$; 0.77 m, 54 H, $[(CH_2)_3Si(OCH_2CH_3)_3]_6$. IR (KBr, cm^{-1}): 3373 ν(N−H); 2975, ν(C−CH_3) 2928, 2886, ν(C−CH_2); 1483, δ(Si−CH_2); 1189, 1162, ν(PN); 1103, 1081, 957 ν(Si−O); 791, 772, δ(C−CH_3). Mass spectrum: *m*/*z* 1455 (M^+), 1410 (M^+ − OCH_2CH_3), 1248(M^+ − OCH_2CH_3- $Si(OCH_2CH_3)_3$).

Synthesis of $N_3P_3[NH(CH_2)_3Si(OEt)_3]_3[N(CH_3)(CH_2)_2CN]_3$ (2). A solution containing 5 g (14.4 mmol) of $N_3P_3Cl_6$, 20.21 g (86.14 mmol) of 3-aminopropyl(triethoxy)silane, and 8.066 mL (86.14 mmol) of $HN(CH_3)(CH_2)_2CN$ with triethylamine (14.43 mL, 104.0 mmol) in 40 mL of toluene was heated under reflux for 6 h. The light-brown precipitate that formed was separated by filtration through a neutral alumina column and the solvent removed from solution. The 3-aminopropyl(triethoxy)silane and triethylamine residues were evaporated under a vacuum at 100 °C. The product was obtained as red-brown oil in quantitative yield.

Elem anal. calcd for $C_{42}H_{93}N_{12}O_9P_3Si_3$ (found): C, 44.6 (42.21); H, 8.88 (9.44); N, 10.62 (12.6). ^{31}P NMR (ppm, $CDCl_3$): 20.8 m, 17.97 m ppm. ^1H NMR (ppm, $CDCl_3$): δ 1.20 m, $[(CH_2)_3Si(OCH_2CH_3)_3]_3$, 36 H; 0.58 m, 27 H, $[(CH_2)_3Si(OCH_2CH_3)_3]_3$. ^{29}Si NMR ($CDCl_3$, ppm): −45.36 ($Si(OCH_2CH_3)_3$). IR (KBr, cm^{-1}): 3354, 3222, ν(N−H); 2974, ν(C−CH_3) 2927, 2885, ν(C−CH_2); 2247.6, ν(CN); 1443, δ(Si−CH_2); 1190, 1167, ν(PN); 1102, 108, 957, ν(Si−O); 791, 770, δ(C−CH_3). Mass spectrum *m*/*z* 1086 (M^+), 1086 (M^+ − $3OCH_2CH_3$-$Si(OCH_2CH_3)_3$), 989 (M^+ − $N(CH_3)$-$(CH_2)_3CN$).

Synthesis N_3P_3 $[NH(CH_2)_3Si(OEt)_3]_3[OC_6H_4(CH_2)CN]_3$ (3). To a solution of $N_3P_3Cl_6$ (5 g, 14.4 mmol) in toluene (20 mL) were added 3-aminopropyl(triethoxy)silane (1.58 g, 7.15 mmol) and triethylamine (14.43 g, 104 mmol) in toluene (50 mL) dropwise at room temperature. The reaction mixture was heated under reflux for 1.5 h. The white precipitate was filtered off and the solution heated at 100 °C to eliminate the 3-aminopropyl(triethoxy)silane and trietylamine residues. Subsequently, a solution of 0.95 mL (7.15 mmol) of $HOC_6H_4CH_2CN$, 11.63 g (35.75 mmol) of potassium carbonate, and 11.52 g (35.75 mmol) of $[NBu_4]Br$ was added and the mixture heated under reflux in acetone for 6 h. The resulting brown solid was removed by filtration, and the solution was chromatographed on neutral alumina and eluted with CH_2Cl_2. The solvent was removed from the eluate, and the red-brown oil was dried under a vacuum for 6 h.

Elem anal. calcd for $C_{51}H_{84}N_9O_{12}P_3Si_3$ (found): C, 46.67 (50.53); H, 8.53 (11.18); N, 9.42 (6.82). ^{31}P NMR($CDCl_3$): 20.89, 18.69. ^1H NMR (ppm, $CDCl_3$): δ 0.97 m, $[(CH_2)_3Si(OCH_2CH_3)_3]_3$, 36 H; 1.19 m, 27 H, $[(CH_2)_3Si(OCH_2CH_3)_3]_3$. IR (KBr, cm^{-1}): 3417, ν(N−H); 2967, ν(C−CH_3); 2934, 2876, ν(C−CH_2); 2240, ν(CN); 1486, δ(Si−CH_2); 1189, 1167, ν(PN); 1104, 1082, 958, ν(Si−O); 793, 771, δ(C−CH_3). Mass spectrum *m*/*z* 1191 (M^+), 1059 (M^+ − $OC_6H_4CH_2CN$), 844 (M^+ − OCH_2CH_3-$Si(OCH_2CH_3)_3$).

Results and Discussion

Synthesis of the Precursors. The analytical data are not perfect for compounds **1**, **2**, and **3**. This can be due to two main factors: the known hydrolytic instability of compunds having the −$Si(OEt)_3$ moiety[8] as well as the incomplete combustion of these types of samples to give a carbon content lower than that calculated. On the other hand, attempts at purification of the oil samples by distillation gave rise to decomposition.

Reaction of $N_3P_3Cl_6$ with $H_2N(CH_2)_3Si(OEt)_3$ in the presence of triethylamine in toluene as a solvent, and at reflux, yields $N_3P_3[NH(CH_2)_3$ $Si(OEt)_3]_6$ (**1**) as a viscous liquid. The ^{31}P NMR spectrum exhibits the typical signal at 0.72 ppm characteristic of $N_3P_3(NR_2)_6$ derivatives[12] (the spectrun is shown in the Supporting Information, S1). The ^1H NMR spectrum exhibited the expected signal of the aminopropyl-(triethoxy)silane[14] group (see the Experimental Section). In the IR spectrum, the ν(PN) ring vibration at 1189 and 1162 cm^{-1},[12] the ν(Si−O) at 791 and 772 cm^{-1},[15c] and the ν(NH) at 3373 cm^{-1} were observed. The mass spectrum of the product shows the expected molecular ion (see the Experimental Section). Other fragments arising from the loss of OCH_2CH_3 and $Si(OCH_2CH_3)_3$ were also observed.

The reaction of $N_3P_3Cl_6$ with $H_2N(CH_2)_3Si(OEt)_3$ and $HN(CH_3)(CH_2)_3CN$ in the presence of triethyl amine and toluene as a solvent results in $N_3P_3[NH(CH_2)_3Si(OEt)_3]_3$-$[NCH_3(CH_2)_3CN]_3$ (**2**) as a red viscous liquid. Unlike compound **1**, the ^{31}P NMR spectrum for the compound **2** showed two resonances at 20.8 and 17.97 ppm (both nearly multiplets) with a relative intensity of 1:2 (see the Supporting Information, S2). In the three stages of substitution in $N_3P_3Cl_6$, two products are expected,[16,17] the geminal and

(14) Caravajal, G. S.; Leyden, D. E.; Quinting, G. R.; Maciel, G. E. *Anal. Chem.* **1988**, *60*, 1776.
(15) (a) Silverman, B. M.; Kristen, K. A.; Wieghaus, A.; Schwartz, J. *Langmuir* **2005**, *21*, 225. (b) Minet, J.; Abramson, S.; Bresson, B.; Sanchez, C.; Montouillout, V.; Lequeux, N. *Chem. Mater.* **2004**, *16*, 3955. (c) Hook, D. J.; Vargo, T. G.; Gardella, J. A.; Litwiler, K. S.; Bright, V. *Langmuir* **1991**, *7*, 142.
(16) Chandrasekar, V. *Inorganic and Organometallic Polymer*; Springer Verlag: Berlin, 2005; Chapter 3; pp 99−101.

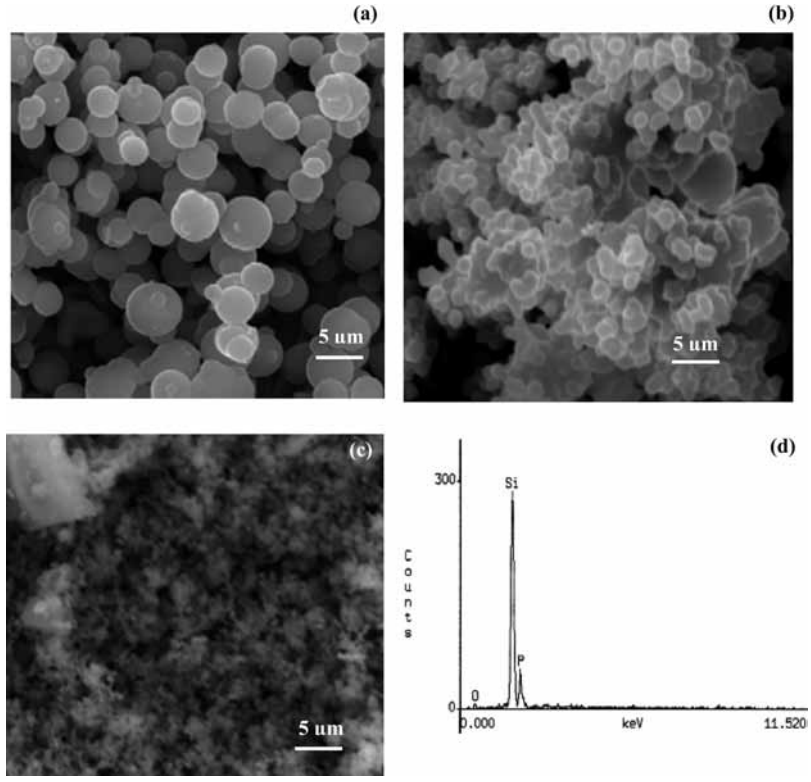

Figure 1. SEM images of the pyrolytic products from precursors (a) **1**, (b) **2**, and (c) **3**. A representative EDAX spectrum is also shown in panel d.

nongeminal compounds. For the gem-cyclo, three well-separated sets of signals are expected, while for the nongeminal substitution, two isomers can be obtained: the 2,4,6-cis with one singlet signals and the 2,4,6-trans with two singlets (or in some cases multiplets) corresponding to an AX_2 system. ^{31}P NMR data for similar structures[18−24] are also in agreement with those of **2**.

This confirms the structure depicted in Scheme 2 for compound **2**. In the ^1H NMR spectrum, the expected signals of the aminopropyl(triethoxy)silane group were observed (see the Experimental Section). The signals of the groups $NCH_3(CH_2)_3CN$ (not shown in the Experimental Section) are normal and appear in the expected range.[16] In their IR spectra, the respective bands corresponding to the ν(PN) ring, ν(Si−O), and ν(NH) vibrations were observed at frequency values similar to those of compound **1**. The ν(CN) band of the group $N(CH_3)(CH_2)_3CN$ was observed at 2248 cm^{-1}. Additionally, the mass spectrum of **2** did not show *m*/*e* peaks corresponding to another substitution product other than that of **2**. The molecular ion was observed as expected (see the Experimental Section) as well as another peaks arising from the loss of $Si(OCH_2CH_3)_3$, OCH_2CH_3, and $N(CH_3)(CH_2)_3CN$ groups.

The reaction of $N_3P_3Cl_6$ with 3 equiv. of $H_2N(CH_2)_3$-$Si(OEt)_3$ in the presence of triethylamine in toluene as a solvent yields, at reflux, the intermediate $N_3P_3[NH(CH_2)_3$ $Si(OEt)_3]_3[Cl]_3$, which reacts with $HOC_6H_4(CH_2)CN$ in acetone and in the presence of K_2CO_3 to give $N_3P_3[NH(CH_2)_3$ $Si(OEt)_3]_3[OC_6H_4(CH_2)CN]_3$ (**3**) as a red-brown oil. Their ^{31}P NMR spectra exhibit, similar to those of **2**, two signals at 20.89 (quartet) and 18.69 (triplet) ppm, with a reltive intensity of 2:1 typical of an AB_2 system (see the Supporting Information, S2). The ^1H NMR spectrum was normal and similar (with respect to the aminopropyl triethoxy silane group signals) to that of **2**.

As previously discussed, this confirms nongeminal substitution and supports the structure proposed in Scheme 2. In their respective IR spectra, the bands corresponding to the ν(PN) ring, ν(Si−O), and ν(NH) vibrations were observed at frequency values similar to those of compounds **1** and **2**. Similarly to **2**, the ν(CN) band of the OC_6H_4-$(CH_2)CN$ group was observed at 2240 cm^{-1}. The mass spectrum showed the expected molecular ion as well as other peaks arising from the loss of fragments OCH_2CH_3, $Si(OCH_2CH_3)_3$, and $OC_6H_4CH_2CN$.

Pyrolysis of the Si Precursors. Pyrolysis of the silicon-containing cyclic trimer phosphazenes **1**, **2**, and **3** results in gray solids in yields of 20−30%. Morphologies of the products depend on the temperature of the pyrolysis and on substituents around the phosphazenes phosphorus. For instance, in comparing the morphology (SEM) of the pyrolytic products at 800 °C from **1**, **2**, and **3**, shown in Figure 1, we observe spherical shapes from **1**, mostly irregular shapes from

(17) Myer, Ch. N.; Allen, Ch. W. *Inorg. Chem.* **2002**, *41*, 60.
(18) Jung, J.-H.; Potluri, S. K.; Zhang, H.; Wisian-Neilson, P. *Inorg. Chem.* **2004**, *43*, 7784.
(19) Wisian-Neilson, P.; Johnson, R. S.; Zhang, H.; Jung, J.-H.; Neilson, R. H.; Ji, J.; Watson, H.; Krawiec, M. *Inorg. Chem.* **2002**, *18*, 4775.
(20) Kumar, D.; Gupta, A. D. *Macromolecules* **1995**, *28*, 6323.
(21) Ainscough, E. W.; Brodie, A. M.; Derwahl, A.; Kirk, S.; Otter, C. A. *Inorg. Chem.* **2007**, *46*, 9841.
(22) Buwalda, P. L.; Steenberger, A.; Oosting, G. E.; Van de Grampel, J. C. *Inorg. Chem.* **1990**, *29*, 2658.
(23) Allcock, H. R.; McIntosh, M. B.; Klingenberg, E. H.; Niepierala, M. E. *Macromolecules* **1998**, *31*, 5255.
(24) Harmjanz, M.; Piglosiewics, I. M.; Scott, B. L.; Burns, C. J. *Inorg. Chem.* **2004**, *43*, 642.

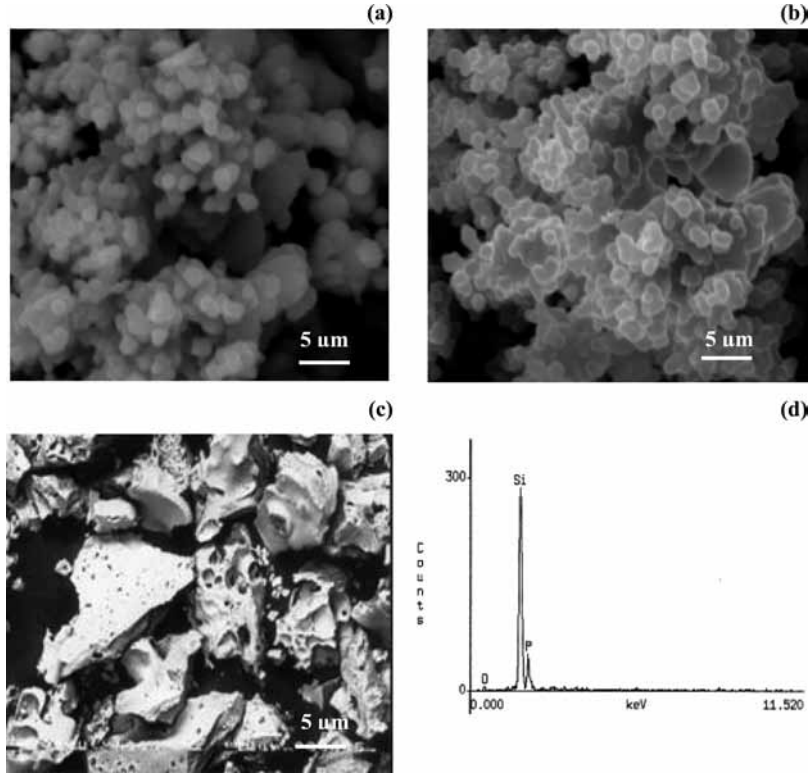

Figure 2. SEM images of the pyrolytic products from precursor **2** at several temperatures: (a) 600 °C, (b) 800 °C, and (c) 1000 °C. A representative EDAX spectrum for these products is also shown in panel d.

the pyrolysis of **2**, and porous materials from **3**. An energy dispersive analysis of X-rays (EDAX) exhibits the presence of silicon, phosphorus, and some oxygen atoms. A representative EDAX spectrum is shown in Figure 1d.

The temperature can also affect the morphology, as is seen in Figure 2 for the products from the pyrolysis of **2** at 600, 800, and 1000 °C. At the highest temperature, a dense and ceramic-like structure is observed. Composition of the materials was investigated by EDAX analysis, powder X-ray diffraction, and IR spectroscopy. EDAX analysis for the pyrolysis products from **1**, **2**, and **3** exhibits similar patterns, confirming the presence of silicon, phosphorus, and trace quantities of oxygen, as is shown in Figures 1d and 2d.

The powder diffraction patterns of the products, shown in Figure 3, are somewhat dependent on the temperature as well as on the nature of the OR groups linked to the cyclotriphosphazene core. Scheme 3 shows the distribution of products after pyrolysis as a function of the temperature for precursors **1**, **2**, and **3**. For example, Figure 3 shows the XRD pattern for **2** at 1000 °C, **3** at 800 °C, and **1** at 1000 °C. The small angle diffraction pattern for **1** at 1000 °C is also shown.

In general, three products from the reaction of SiO_2 and P_2O_5 were observed, that is, crystalline $Si_5(PO_4)_6O$ and SiP_2O_7 and a glassy amorphous phase, $Si_5(PO_4)_6O/3SiO_2 \cdot 2P_2O_5$. It is known that the reaction of SiO_2 and P_2O_5 or SiO_2 with H_3PO_4 results in the formation of $Si_5(PO_4)_6O$, SiP_2O_7, or the glassy $Si_5(PO_4)_6O/3SiO_2 \cdot 2P_2O_5$, depending on the temperature and on the conditions of the reaction.[25a−e] However, the as-obtained materials are microcrystalline samples and not nanostructured as those obtained here.

The X-ray diffraction pattern for **3** at 800 °C exhibits peaks corresponding to $Si_5(PO_4)_6O$[25b] (arrows), the glass $Si_5(PO_4)_6O/3SiO_2 \cdot 2P_2O_5$[25−27] (circles), and SiP_2O_7[25c,d] (triangles), see Figure 3b. In contrast, the diffraction data for **2** at 800 °C exhibit only peaks corresponding to $Si_5(PO_4)_6O$, Figure 3c. The pyrolysis of **1** at 1000 °C, however, results in several crystalline forms of SiO_2, as shown in Figure 3a. This is in good agreement with the previously reported decomposition of SiP_2O_7 at temperatures above 1000 °C,[25b−d] to give SiO_2 and P_2O_5. A hexagonal MCM-41 SiO_2 phase was also formed, as is seen from the low-angle XRD pattern shown in Figure 3d, similar to a recent report of SiP_2O_7 grafted to MCM-41.[25f]

From Scheme 1, it can be seen that $Si_5(PO_4)_6O$ is present in the pyrolysis of precursors **1**, **2**, and **3** at all temperatures assayed. In contrast, the pyrophosphate salt SiP_2O_7 was present only for precursor **3** at 800 °C. The glass of composition, $Si_3PO_4/3SiO_2/2P_2O_5$, was also observed in the pyrolysis of **3** at all of the temperatures examined. This

(25) (a) Li, D.; Bancraft, G. M.; Kosrai, M.; Fleet, M. E.; Feng, X. H.; Tan, K. H. *Am. Mineral.* **1994**, *79*, 785. (b) Poojaray, D. M.; Borade, R. B.; Clearfield, A. *Inorg. Chim. Acta* **1993**, *208*, 23. (c) Poojaray, D. M.; Borade, R. B.; Campbell, F. L.; Clearfield, A. *J. Solid State Chem.* **1994**, *112*, 106. (d) Tillmanns, E.; Gebert, W. *J. Solid State Chem.* **1973**, *7*, 69. (e) Nishiyama, N.; Kaihara, J.; Nishiyama, Y.; Egashira, Y.; Ueyama, K. *Langmuir* **2007**, *23*, 4746. (f) Kovalchuk, V.; Sfihi, H.; Korchev, A. S.; Kovalenko, A. S.; II'in, G.; Zaitzev, V. N.; Fraissard, J. *J. Phys. Chem.* **2005**, *109*, 13948.
(26) Suehara, S.; Konishi, T.; Inoue, S. *Phys. Rev. B*, **2006**, *73*; DOI: 10.1103/PhysrevB73.092203.

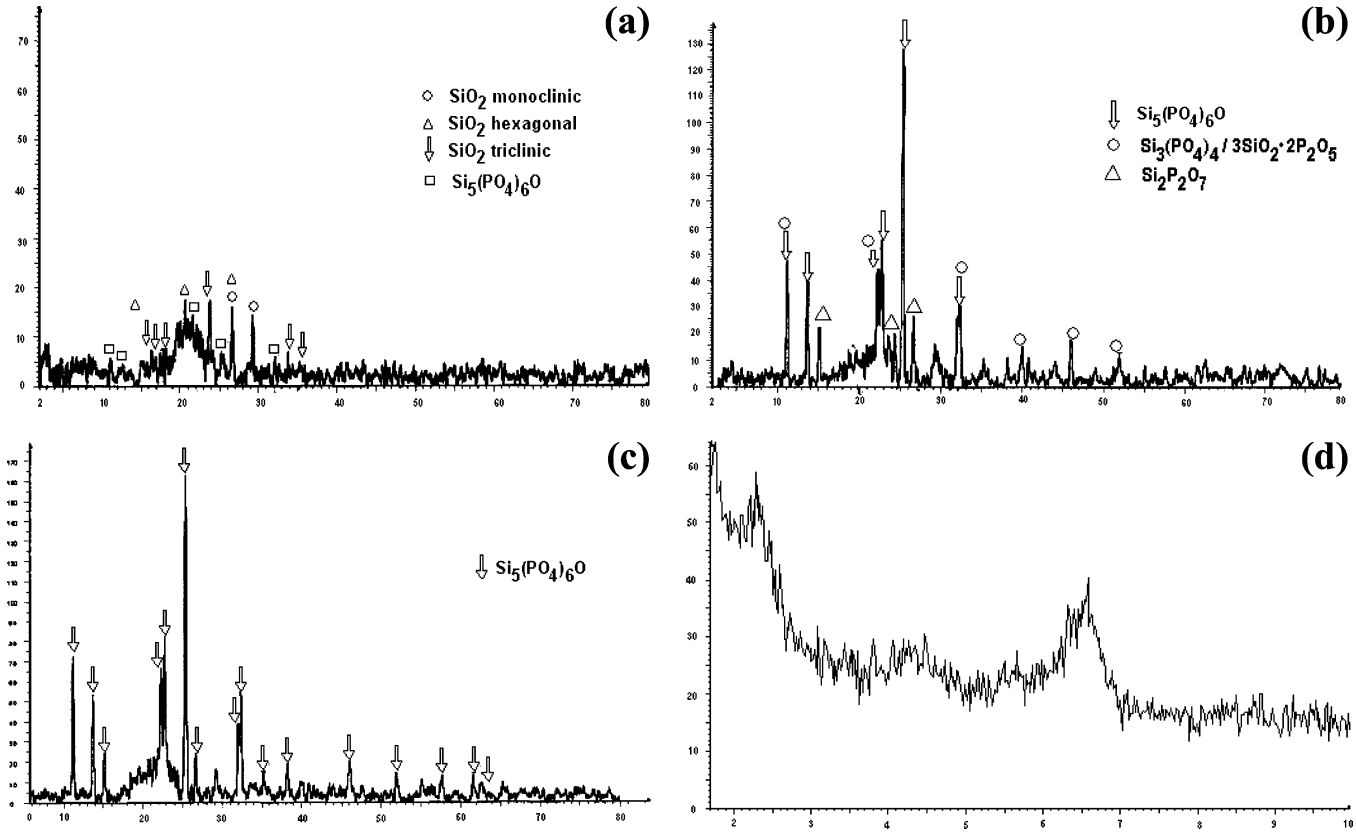

Figure 3. X-ray powder diffraction data for the pyrolytic products from (a) **1** at 1000 °C, (b) **3** at 800 °C, and (c) **2** at 800 °C. (d) SAXRD pattern for **1** at 1000 °C.

Scheme 3. Schematic Representation of the Distribution of Products from Pyrolysis of Precursors **1**, **2**, and **3** at Several Temperatures

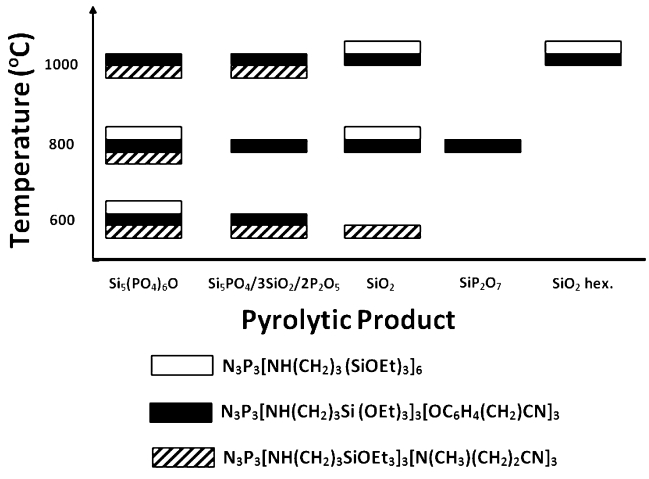

product was only observed at 600 and 1000 °C for the pyrolysis of **3**. Conversely, SiO_2 was obtained for all three precursors but at only at a single temperature for each one. Amorphous and crystalline materials of composition $M_xO_y/nSiO_2/mP_2O_5$ are interesting due to third-order nonlinear optical susceptibility properties, when M_xO_y is a transition metal oxide,[26] and bioactive ceramic behavior is observed when the composition M_xO_y is Na_2O, MgO, or CaF_2.[27,28]

The microspheres formed in the pyrolysis of precursor **1** at 800 °C are the first generated using phosphazenes as a template.[10] The resulting spheres were further investigated by means of TEM. Figure 4a−f displays the micrographs of a sample after calcination at 800 °C.

The core−shell spheres structure of the aggregate nanoparticles of $Si_5(PO_4)_6O/SiO_2$ was clearly observable in the case of the pyrolysis of precursor **3**, as is shown in Figure 4e,f. For all of the cases, the core−shell structure was also corroborated from energy dispersive X-ray spectroscopy data and using a method previously reported[29,30] based on the core/shell contents, in this case, from the Si/P contents of SiO_2 spheres coated with $Si_5(PO_4)_6O$. As is illustrated for the pyrolytic product from **1** and **2**, the electron diffraction image indicates somewhat amorphous material in all of the cases.

BET Studies. BET studies were conducted on compounds **1**, **2**, and **3** to quantify the degree of porosity observed by SEM. The N_2 adsorption isotherms of the pyrolytic product from **1** indicate the presence of mesopores with a mean diameter of 24.4 nm, as measured from the pore size distribution curve with a relatively low surface area of 3.2 $m^2\ g^{-1}$. Similar observations are found for the pyrolytic products from **2** and **3** with values of mean pore size of 52.1 and 19.9 nm, respectively, with corresponding surface areas of 2.0 and 2.3 $m^2\ g^{-1}$. These values are less than those found for $SiO_2 \cdot P_2O_5 \cdot M_xO_y$ glasses.[32]

(27) Vallet-Regi, M.; Roman, J.; Padilla, S.; Doadrio, J. C.; Gil, F. J. *J. Mater. Chem.* **2005**, *15*, 1353.
(28) Perez-Pariente, J.; Balas, F.; Vallet-Regi, M. *Chem. Mater.* **2000**, *12*, 750.

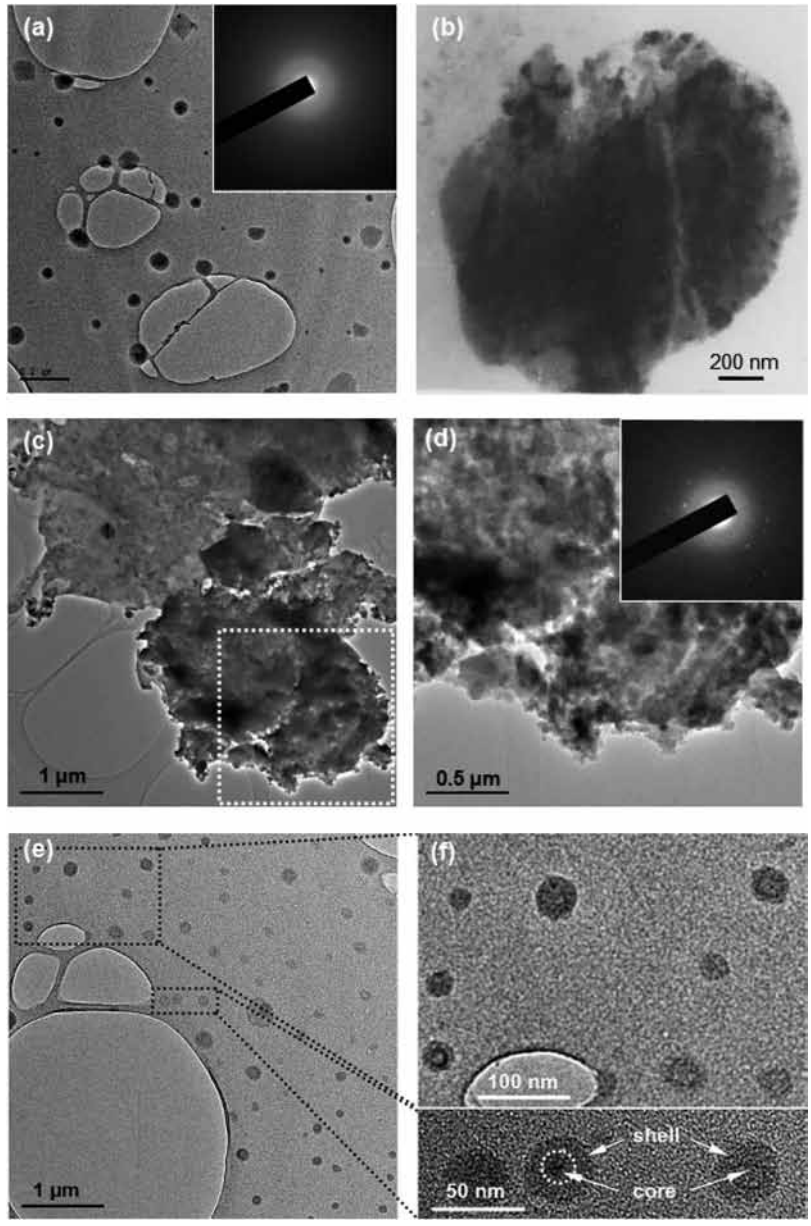

Figure 4. TEM images of pyrolytic products from a and b, **1**; c and d, **2**; and e and f, **3**, at 800 °C. Insets to b and d are the respective electron diffraction images patterns.

Possible Formation Mechanism of the Si Nanostructured Materials. Some insight into the mechanism of formation of the nanostructured silicon materials from the silylated cyclotriphosphazene precursors can be obtained from the TGA/DSC results in air, shown in Figure 5a. TGA and DSC for the pyrolytic products from **2** and **3** exhibit similar behavior (see the Supporting Information, S3−S11).

The initial weight loss of 9.31% is attributed to the volatilization of NO_2 by oxidation of the nitrogen content of the cyclic trimer. The second weight loss corresponds to the carbonization of the organic matter arising from the $N(CH_3)(CH_2)_3CN$ groups. The following weight loss is attributed to a loss of CO_2 from carbonization of the remaining organic matter, that is, the $Si(OEt)_3$ groups. The 41.19% pyrolytic residue is close to that expected for SiO_2, 39.76% $Si_5(PO_4)_6O$. It is at this point that the cyclotriphosphazene acts as a hybrid organic−inorganic template in the solid state during the formation of the silicon nanoparticles. This implies that, upon initial heating, a cross-linked structure involving cyclotriphosphazene linked by Si−O−Si bridges is formed. In fact, organosilicon derivatives of cyclotriphosphazene undergo cross-linking of the ring upon heating.[33] The organic moiety, after calcination, produces holes in the cross-linked structures, which permit agglomeration of the silicon-containing particles. The inorganic PN backbone of the polyphosphazenes in the presence of oxygen provides phosphorus atoms for the formation of the corresponding

(29) Hanprasopwattana, A.; Srinivasan, S.; Sault, A. G.; Datye, A. K. *Langmuir* **1996**, *12*, 3179.
(30) Haukka, S.; Lakomas, E. L.; Jyha, O.; Vilhunen, J.; Hornytzkyj, S. *Langmuir* **1993**, *9*, 3497.
(31) Uma, T.; Mogami, M. *Chem. Phys.* **2006**, *98*, 382.
(32) Raman, J.; Padilla, S.; Vellet-Regi, M. *Chem. Mater.* **2003**, *15*, 708.
(33) Allcock, H. R.; Brennan, D. J. *J. Organomet. Chem.* **1988**, *341*, 231.

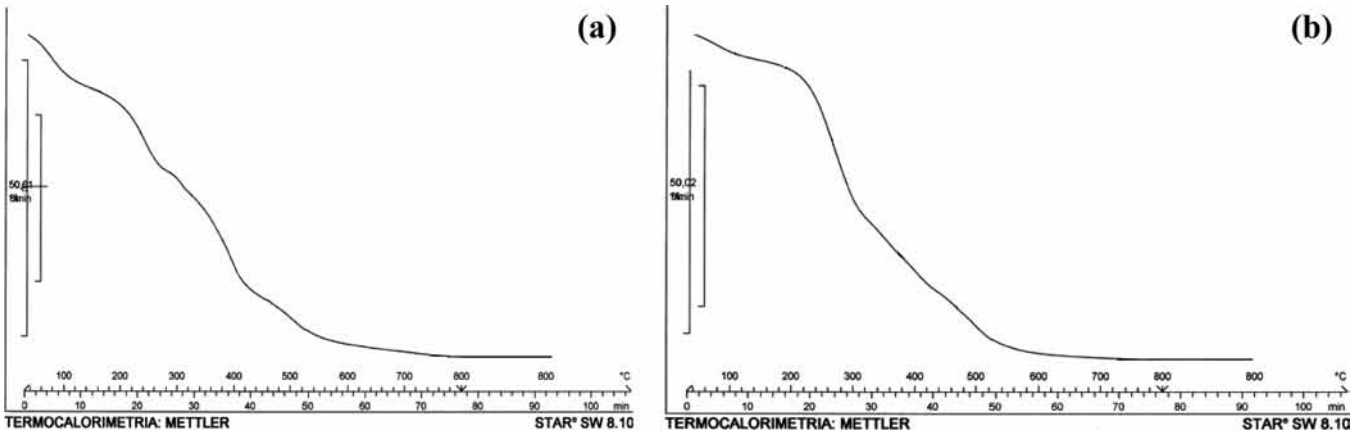

Figure 5. TGA curve for the pyrolytic product from precursor **1**: (a) in air and (b) in N_2.

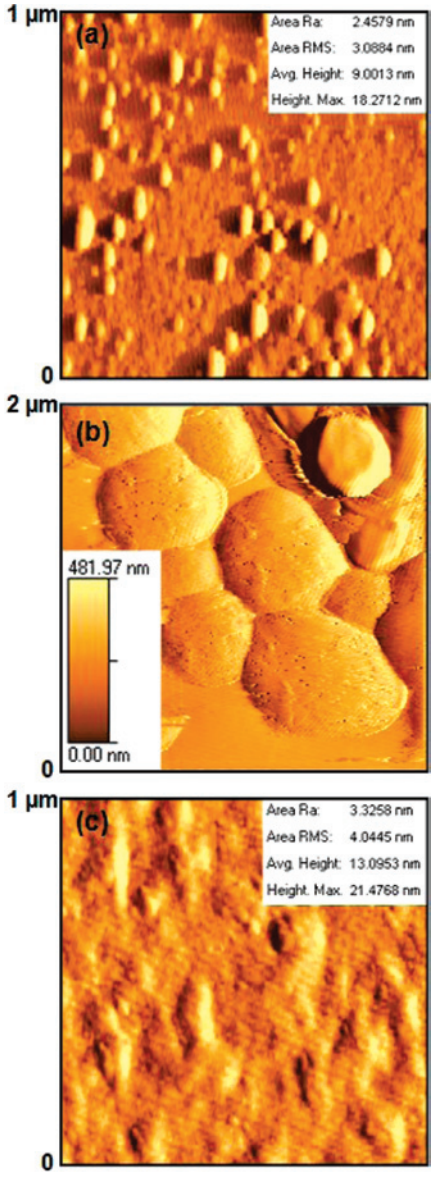

Figure 6. AFM images of the pyrolytic products from (a) precursor **1**, (b) precursor **2**, and (c) precursor **3**.

phosphorus oxides, which react with the SiO_2 to form $Si_5(PO_4)_6O$ (or $Si_5(PO_4)_6O/3SiO_2 \cdot 2P_2O_5$ or SiP_2O_7 in some cases).

DSC curves also performed in air (see the Supporting Information, S9−S11) are also in agreement with this proposed mechanism. In fact, the exothermal peaks at 250 and 300 °C can be assigned to the carbonization of the organic matter. Similar exothermic peaks have been observed during the oxidation of organometallic complexes.[35−37]

Interestingly, the TGA curve in N_2 (see Figure 5b) exhibits similar loss weight patterns. According to the equation for the combustion of the trimer **1**,

$$2N_3P_3[NH(CH_2)_3Si(OEt)_3]_6 + 29.5O_2 \rightarrow Si_5(PO_4)_6O + 7SiO_2 + 108CO_2 + 18NO_2$$

the oxygen content necessary for the formation of SiO_2 and $Si_5(PO_4)_6O$ in the absence of air (N_2 in this instance) can be partially supplied by the oxygen from the $Si(OEt)_3$ groups, but the quantity available is insufficient for the total carbonization of the organic matter.

Thus, this mechanism is in agreement with those proposed for the formation of nanostructured metal foams from the thermal decomposition of bi(tetrazolato)amine complexes[37] and from the thermal decomposition of $[Fe(\eta\text{-}C_5H_4)_2(SiRR')]_n$ polymers.[38]

IR Spectra. The IR and Raman spectra of the products from the reactions of SiO_2 with P_2O_5 have been studied in detail.[39] All pyrolytic products from **1**, **2**, and **3** exhibit absorptions at 1180−1050 (vs, broad), 800−680 (w), and 490 (s, broad), which are typical of some of the reaction products of SiO_2 with P_2O_5, that is, crystalline $Si_5(PO_4)_6O$, SiP_2O_7, or the amorphous glass $Si_5(PO_4)_6O/3SiO_2 \cdot 2P_2O_5$.

Surface Morphological Studies of Deposited Precursors. Suitable AFM studies of the trimer samples were achieved by dissolving a dichloromethane solution followed by dropwise deposition onto a silicon wafer, evaporation at

(34) Vallet-Regi, M.; Roman, J.; Padilla, S.; Doadrio, J. C.; Gil, F. J. *J. Mater. Chem.* **2005**, *5*, 1353.
(35) Laite, E. R.; Carreño, N,L.; Longo, E.; Pontes, F. M.; Barison, A.; Ferreira, A. G.; Maniette, Y.; Varela, A. G. *Chem. Mater.* **2002**, *14*, 3722.
(36) Boxall, D. L.; Kenic, E. A.; Lukahart, C. M. *Chem. Mater.* **2002**, *14*, 1715.
(37) Tappan, B. C.; Huynhn, M. H.; Hysley, A.; Chavez, D. E.; Luther, E. P.; Mang, J. T.; Son, S. F. *J. Am. Chem. Soc.* **2006**, *128*, 6589.
(38) Petersen, R.; Foucher, D. A.; Tang, B. Z.; Lough, A.; Raju, N. P.; Greedan, J. E.; Manners, I. *Chem. Mater.* **1995**, *7*, 2045.

room temperature, and pyrolysis at 800 °C. For trimer **1**, separated grains of an average height of ∼20 nm were observed, as is shown in Figure 6.

The pyrolytic product from trimer **2** is observed to form large islands with varied sizes (from 50 nm to 180 nm) that nucleate and grow progressively in three dimensions, as is shown in Figure 6b. In several cases, these islands are either isolated or joined forming a chain, shown in Figure 6b. For the pyrolytic product from trimer **3**, a more uniform coverage of the nanostructures is observed, as is shown in Figure 6c.

Conclusions

Siliceous nanostructured materials are accessible in a wide range of morphologies and compositions through the solid-state pyrolysis of new precursors **1**, **2**, and **3**. Both the morphology and composition of the nanostructured products are strongly dependent on the nature of the groups around the phosphazenic ring and on the temperature of the pyrolysis. Oxidation of the phosphorus of the polymeric chain and of the silicon from the siloxane groups gives P_2O_5 and SiO_2, respectively, which react, resulting in silicon phosphates in their crystalline phases $Si_5(PO_4)_6O$ and SiP_2O_7 or in an amorphous phase such as the glass $Si_5(PO_4)_6O/3SiO_2 \cdot 2P_2O_5$. These nanoparticles are grown inside the vacancies, which are formed by carbonization of the organic matter, giving rise to nanostructured silicon compounds.

AFM images evidence increasing grain density on the surface of the deposition upon going from pyrolytic precursor **1** to **3**. This new technique shows promise for being a flexible, general approach to the formation of a range of nanostructured siliceous pyrophosphate materials not currently accessible by other methods.

Acknowledgment. The authors thank Dr. Paulo Araya (Faculty of Physics and Mathematics, Universidad de Chile) for the BET measurements and Dr. Calum Dickinson for the TEM measuremets. Financial support from FONDECYT, project 1085011, is also acknowledged.

Note Added after ASAP Publication. Due to production errors, this article was published ASAP on November 1, 2008, with minor text errors and incorrect versions of Scheme 3 and Figures 4 and 6. The corrected article was published on November 13, 2008.

Supporting Information Available: ^{31}P NMR spectrum for **1**, **2**, and **3**; TGA curves for **2** and **3** in air and N_2; and DSC curves for **1**, **2**, and **3** in air and nitrogen. This material is available free of charge via the Internet at http://pubs.acs.org.

IC8009805

(39) (a) Shibata, N.; Horigudhi, M.; Edahiro, T. *J. Non-Cryst. Solids* **1981**, *45*, 115. (b) Wong, J. *J. Non-Cryst. Solids* **1973**, *20*, 83.